Available online at www.sciencedirect.com

SciVerse ScienceDirect

Ceramics International 39 (2013) 1931–1942

CERAMICS INTERNATIONAL

www.elsevier.com/locate/ceramint

Microstructure and mechanical properties of WC–40vol%Al_2O_3 composites hot pressed with MgO and CeO_2 additives

Haixia Qu[a], Shigen Zhu[a,b,*], Ping Di[c], Chenxin Ouyang[a,b], Qian Li[a]

[a]College of Mechanical Engineering, Engineering Research Center of Advanced Textile Machinery, Ministry of Education, Donghua University, Shanghai 201620, PR China

[b]College of Material Science and Engineering, Donghua University, Shanghai 201620, PR China

[c]Analysis and testing center, Donghua University, Shanghai 201620, PR China

Received 11 June 2012; received in revised form 15 August 2012; accepted 15 August 2012
Available online 23 August 2012

Abstract

Effects of trace amount of MgO and CeO_2 additives on the microstructure and mechanical properties of the WC–40 vol%Al_2O_3 composites prepared by hot pressing were investigated. The results showed that both the WC–Al_2O_3 composites doped with 0.1 wt%MgO and 0.1 wt%CeO_2 separately, and the WC–Al_2O_3 composites doped with 0.05 wt%MgO and 0.05 wt%CeO_2 together, possessed the refined microstructure and enhanced mechanical properties compared with that of the undoped WC–Al_2O_3 composites. Trace MgO mainly acted as an effective grain growth inhibitor for the WC–Al_2O_3 composites and trace CeO_2 suppressed the decarburization of WC, promoted the microstructural refinement and improved the interface coherence of the WC matrix and Al_2O_3. When 0.05 wt%MgO and 0.05 wt%CeO_2 were added to the WC–Al_2O_3 composites, the synergistic effect of MgO and CeO_2 resulted in the achievement of a relative density of 99.04% with an excellent Vickers hardness of 18.18 GPa, combining a fracture toughness of 10.14 MPa $m^{1/2}$ with an acceptable flexural strength of 1158.38 MPa.

Keywords: A. Hot pressing; B. Microstructure-final; C. Mechanical properties; D. WC–Al_2O_3 composites

1. Introduction

The cemented carbides (WC–Co) with the attractive characteristics of high hardness and good fracture toughness are widely used for a variety of machining, cutting, drilling and other applications [1]. They consist of a high volume of hard tungsten carbide (WC) phase embedded within the soft cobalt (Co) binder phase. However, metallic Co binders are not economically attractive and will result in reduced hardness and corrosion/oxidation resistance, enhance grain growth due to the rapid diffusion in the liquid phase [2,3]. In addition, the continuing trend of saving the rare, expensive and strategic resource of Co requires the development of novel WC matrix materials with high mechanical properties. In the recent years, WC–TiC [4], WC–ZrO_2 [5], WC–$FeCl_3$ [6], WC–MgO [7,8] composites have been consolidated to save the resource of Co.

Nowadays, a new composite material, WC–Al_2O_3 composite has been successfully hot pressed possessing a combination of attractive mechanical properties including low density, high Vickers hardness, fracture toughness and flexural strength [9]. These excellent properties along with low cost make WC–Al_2O_3 composites potentially useful for structural and coating applications.

As for ceramics materials, the intrinsic low fracture toughness and modest flexural strength of them, however, limit the applicability of them under severe conditions such as for high speed cutting tools. Considerable effects have been made during recent years to overcome their inherently low fracture toughness and the declining strength by the dispersion of additives.

*Corresponding author at: Donghua University, Engineering Research Center of Advanced Textile Machinery, Ministry of Education, College of Mechanical Engineering, Renmin Road Songjiang District, Shanghai 201620, PR China. Tel./fax: +86 21 6779 2813.
E-mail address: sgzhu@dhu.edu.cn (S. Zhu).

0272-8842/$ - see front matter © 2012 Elsevier Ltd and Techna Group S.r.l. All rights reserved.
http://dx.doi.org/10.1016/j.ceramint.2012.08.043

For example, magnesia (MgO) is added to Al_2O_3 ceramics to improve the mechanical properties by roughening grain boundary and inhibiting abnormal grain growth. Ever since Coble's [10] pioneering work in the early 1960 s, it is well known that MgO acts as a grain growth inhibitor in alumina by pinning down the grain boundary migration. Various mechanisms such as second phase, solute segregation have been proposed [11]. Berry et al. have summarized four main views about the exact role of MgO acting as the solid solution [12]. For most of these models, an absolutely pure Al_2O_3 is assumed.

In addition, MgO has been added to the WC matrix as a second phase to consolidate WC–MgO composites with excellent mechanical properties [7,8], indicating that MgO is an effective additive in toughening the WC matrix ceramic materials. However, few papers available investigating the effects of MgO as a solid solution additive on the grain size, relative density, microstructure and mechanical properties of WC–Al_2O_3 composites. So when we consolidate WC–Al_2O_3 composites, MgO is certainly considered as an addition to improve the properties of it.

In the case of WC matrix ceramics, it is reported that adding an optimum range of Sm, Y, Ce, CmPr or LaCe rare earth metals or metal mixtures can improve the flexural strength of YT15 (WC–15 wt%TiC–6 wt%Co) cemented carbide [13]. Pan's results show that adding small amount of rare earth oxides raise the bending strength and wear resistance, and increase the corrosion resistance of cemented carbide [14]. Xiao et al. [15] report that addition of both Y_2O_3 and NbC could improve the fracture toughness of WC–10Co alloys without compromising its hardness. Ma and Zhu [16] investigate the influence of La_2O_3 addition on hardness, flexural strength and microstructure of hot pressed WC–MgO bulk composites, and indicate that the La_2O_3 addition could not only improve the flexural strength of WC–MgO bulk composites but also enhance the Vickers hardness. In addition, grain boundaries could also be strengthened by doping rare earth dopants in Al_2O_3 [17].

From the aforementioned information, it could be speculated that the rare earth oxides must have some positive effects on the WC–Al_2O_3 composites and could be used to improve the mechanical properties of it.

According to the previous investigations, although the hot pressing of MgO doped WC–Al_2O_3 composite has been reported earlier by Endo et al. [18], the effects of MgO on the density, microstructure and mechanical properties should be investigated in details. There is no report available on the WC–Al_2O_3 composites with enhancement of mechanical properties like HV, K_C, σ with rare earth oxides.

In this paper, WC–Al_2O_3 composites with MgO and CeO_2 doped both separately and together are consolidated for the first time and the promotive effects of MgO and CeO_2 additives on the microstructure and mechanical properties of WC–Al_2O_3 composites are evaluated and reported.

2. Experimental procedure

99.5% purity commercial powders (Sinopharm Chemical Reagent Co. Ltd.) of WC (74 μm), α-Al_2O_3 (74 μm), MgO (48 μm) and CeO_2 (16 μm) were used in this study. The powder systems of WC–40 vol%Al_2O_3–$x$wt%MgO and WC–40 vol%Al_2O_3–$x$wt%CeO_2 (x=0, 0.05, 0.1, 0.25, 0.5, 1 wt%) were premixed and ball milled using a QM-1SP4 planetary ball milling machine under argon gas atmosphere for 50 h, respectively. The ball to powder weight ratio was 10:1 and the rotation speed of the mill was 350 revolutions per minute (rpm). Both the vial and milling balls (10 mm in diameter) were made of cemented carbide materials. The particle size of the as milled powders varied from 47 to 573 nm in diameter.

The as milled powders were hot pressed using a vacuum hot pressing furnace (ZT-40-20YB, Shanghai Chen Hua Electric Furnace Co. Ltd., China) at 1540 °C under a pressure of 39.6 MPa (applied already from the start) in a vacuum (about 1.3×10^{-1} Pa) atmosphere for 90 min. The heating rate of the hot pressing was 10 °C/min. Carbonic paper with a thickness of 0.2 mm was used to prevent adhesion between powders and the die/mould. The thermoelectric couple and infrared thermometer were selected to measure the temperature, located in the surface of the mold.

The hot pressed samples were ground and polished by standard ceramographic methods and then etched in a Murakami's reagent consisting of $Fe_3[K(CN)_6]$ (10 g), KOH (10 g) and distilled water (100 ml) for 5 min to expose the grain boundary of WC. Phase identification of the polished samples were investigated by X-ray diffraction (XRD) using a D/max-2550PC (Rigaku Co., Japan) X-ray diffractometer with a Cu K_α radiation (λ=0.15418 nm) at 400 kV and 200 mA. X-ray Photoelectron Spectroscopy (XPS) measurements were carried out on the as milled WC–40 vol%Al_2O_3–0.1 wt%CeO_2 powders and the polished surfaces of hot pressed WC–40 vol%Al_2O_3–0.1 wt%CeO_2 bulk composites using XSAM800 (Kratos, UK) multifunctional surface analysis electronic spectrometer with a Al K_α source (1486.6 eV) at 12 kV and 15 mA. The pressure inside the vacuum chamber was 2×10^{-7} Pa. Spectra were analyzed using XPSPEAK41 software. The microstructure of the polished samples was characterized by S-4800 (Hitachi Co., Japan) field emission scanning electron microscope (FE-SEM) and Nanoscope IV (Veeco Co., USA) scanning probe microscope (SPM). Chemical composition was examined by energy dispersive spectroscope (EDS). The polished and etched samples were characterized by JSM-5600LV (JEOL Co., Japan) scanning electron microscope (SEM). The WC grain size and Al_2O_3 particle size were estimated, respectively, by the linear intercept method. For each sample, at least three images were taken of the microstructure; in each image a minimum of five line segments were assessed. The fracture surfaces of the sintered samples were observed by S-3400 N (Hitachi Co., Japan) scanning electron microscope (SEM).

The densities of the sintered samples were measured using water immersion method in accordance with Archimedes' principle. The hardness of sintered specimens (the average of 10 indentations) was determined using a HVS-50Z Vickers indenter with a load of 30 kg and a dwell time of 10 s. The crack shapes of the specimen determined by repeated surface polishing were confirmed to be Palmqvist crack pattern and in accordance with the Shetty's model, so the fracture toughness (K_C) calculations were based on the crack length measurement of the radial crack pattern produced by Vickers indentations according to the formula estimated by Shetty et al. [19]. The fracture toughness values were derived from the average of 10 measurements. The flexural strength of sintered samples was measured by the three-point flexural test method at room temperature according to the ASTM B312 standard. The samples were cut, ground and polished into $3 \times 5 \times 15\ mm^3$ specimens. The three-point flexure tests were carried out on a WDW-100 (Changchun kexin experimental equipment Co. Ltd., China) test machine with a span of 10 mm and cross-head speed of 0.01 mm/min. The fracture strength of sintered samples (the average of six tests) was calculated using

$$\sigma = 3PL/2t^2w \quad (1)$$

where σ (MPa) is the flexural fracture strength, P (N) is the force required to rupture, L ($L=10$ mm) is the length of the span of fixture, w ($w=5$ mm) is the width of the specimen, and t ($t=3$ mm) is the thickness of the specimen.

3. Results and discussion

3.1. Investigation of the optimum contents of MgO and CeO_2 added separately to the WC–40vol%Al_2O_3 composites

To obtain the optimum contents of MgO and CeO_2 added to the WC–Al_2O_3 composites, the WC–Al_2O_3 composites doped with MgO and CeO_2, respectively, were hot pressed at 1540 °C for 90 min according to the best hot pressing parameters reported in [9].

Fig. 1 shows the effects of the content of MgO on the grain size of WC, the relative density, Vickers hardness and fracture toughness of the WC–40 vol%Al_2O_3–MgO composites. From Fig. 1a it can be seen that small amount of MgO was beneficial to the improvement of relative densities of WC–40 vol%Al_2O_3–MgO composites. The relative density increased initially to the maximum value when the MgO content reached to 0.1 wt%, then it decreased with the increasing MgO content. The grain size of WC initially decreased from 3.92 μm to 2.3 μm when the MgO content increased from 0 to 0.1 wt%, then increased correspondingly with the increasing content of MgO. From Fig. 1b, it could be observed that the Vickers hardness and fracture toughness of WC–40 vol%Al_2O_3–MgO composites were significantly improved with the addition of MgO. When the MgO content was 0.1 wt%, both the Vickers hardness and fracture toughness reached to the maximum values of 17.6 GPa and 9.59 MPa $m^{1/2}$, respectively. With the increasing content of MgO, the Vickers hardness and fracture toughness were still higher than that of undoped WC–40 vol%Al_2O_3 composites, however, following a decreasing trend. It was indicated that the optimum MgO content was 0.1 wt%; an excessive addition of MgO (0.25 wt%–0.1 wt%) resulted in the decreasing relative density, increasing WC grain size and decreasing mechanical properties.

According to the above results, it could be indicated that, MgO, as a sintering additive, had a key role in improving the densification and mechanical properties of the WC–40 vol%Al_2O_3 composites. MgO addition acted to increase the rate of densification directly through a raising diffusion coefficient and decrease the rate of grain growth during sintering through a lowering surface diffusion coefficient. Meanwhile, MgO addition could also lower the grian boundary mobility [12]. These were the main reasons for the high relative density, refined WC grain size and enhanced mechanical properties of the WC–40 vol%Al_2O_3 composites doped with 0.1 wt% MgO. However, excessive amount of MgO addition deteriorated the mechanical properties, as shown in Fig. 1.

The influence of CeO_2 content on the grain size of WC, the relative density, Vickers hardness and fracture toughness of WC–40 vol%Al_2O_3–CeO_2 composites were illustrated in

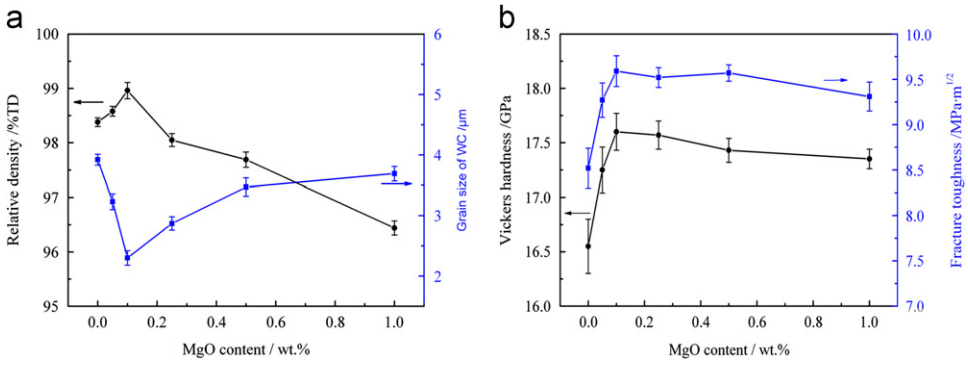

Fig. 1. (a) Relative density and grain size of WC, (b) Vickers hardness and fracture toughness of the MgO doped WC–40 vol%Al_2O_3 composites as a function of the MgO content.

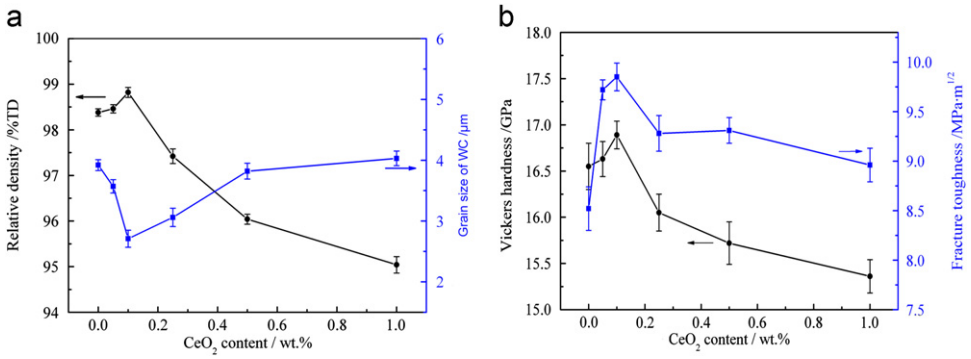

Fig. 2. (a) Relative density and grain size of WC, (b) Vickers hardness and fracture toughness of the CeO_2 doped WC–40 vol%Al_2O_3 composites as a function of the CeO_2 content.

Fig. 2. It was obvious that CeO_2 was also an effective addition to improve the properties of WC–40 vol%Al_2O_3 composites. When the CeO_2 content was smaller than 0.1 wt%, the relative density increased and the grain size of WC decreased. Doping of 0.1 wt%CeO_2 in WC–40 vol%Al_2O_3 composites increased the relative density from 98.38% up to 98.82%, however, further addition of CeO_2 resulted in sharp decrease of relative density, as shown in Fig. 2a. For undoped WC–40 vol%Al_2O_3 composites, the grain size of WC was 3.92 μm, the addition of 0.1 wt% CeO_2 significantly decreased the grain size of WC to 2.71 μm. However, it was found that the WC grain size increased with the increasing CeO_2 content in the WC–40 vol%Al_2O_3–CeO_2 system, when the CeO_2 content increased to 1 wt%, the WC grain size reached 4.03 μm, 1.5 times larger than that of the 0.1 wt% CeO_2 doped WC–40 vol%Al_2O_3 composites. From Fig. 2b, it can be seen that the Vickers hardness and fracture toughness of WC–40 vol%Al_2O_3–CeO_2 composites were significantly increased with the addition of 0.05 wt%CeO_2 and 0.1 wt%CeO_2, further addition of CeO_2 resulted in lowered Vickers hardness and fracture toughness values. It was clear that when the CeO_2 content exceeded 0.1 wt%, the Vickers hardness of WC–40 vol%Al_2O_3–CeO_2 composites were lower than that of the undoped one. It means that a critical content of CeO_2 could restrain the WC grain growth and improve the density of WC–40 vol%Al_2O_3 composites effectively, above which grain growth would occur, and the relative density would decreased, resulting in the reduced Vickers hardness and fracture toughness.

The ions of additives segregation to grain and phase boundaries was quite general phenomenon widely observed in ceramics [20,21], and was particularly important to diffusion process during sintering of ceramics. The MgO and CeO_2 additives dispersed in the WC–40 vol%Al_2O_3 composites may also predominantly occupied the intergranular positions due to the mismatch of the ionic radii and strain energy of CeO_2, Al_2O_3, and WC.

Although the grain boundaries in pure Al_2O_3 were reported to carry a positive charge [22], the segregation of Ce on Al_2O_3 boundaries was not explicable by the space charge model since tetravalent and isoelectric trivalent solutes in Al_2O_3 had effective charges of +1 and 0, respectively. It was argued that due to large differences in ionic radii, the solute misfit strain energy was the dominating driving force for the segregation of Ce to the grain boundaries [23]. A similar behavior was reported for the segregation of Si, Zr and La solutes on grain boundaries in Al_2O_3, where ion misfit strain energy seemed to be the driving force for segregation [24]. And Su et al. reported the La_2O_3 and Y_2O_3 existed at the grain boundaries of Al_2O_3 composites, where the concentration distribution of La_2O_3 and Y_2O_3 were thermodynamically non-equilibrium[25], owing to the discrepancy of ionic radii between La^{3+}, Y^{3+} and Al^{3+} (r^{3+}_{La}= 0.103 nm, r^{3+}_{Y}=0.09 nm, r^{3+}_{Al}=0.053 nm). Ma and Zhu reported that the La_2O_3 added into the WC–MgO composites could accumulate along these interfaces between the MgO toughening particulates and WC matrix, where the atomic arrangement was irregular, because of the so-called "adsorption effect"[16].

The MgO and CeO_2 doped WC–Al_2O_3 powders were sufficiently mixed during the high energy ball milling process, so the MgO and CeO_2 could segregate in both grain boundaries (WC–WC, Al_2O_3–Al_2O_3) and phase boundaries (WC–Al_2O_3).

Segregation in grain boundaries could influence the grain boundary complexion and interfacial kinetics, and the critical driving force (Δg_c) of grains could be changed by the additives. Harmar [26] has well explained the interfacial kinetic engineering and the Dillon–Harmer [27] complexion types I–VI. A clean boundary was classed as complexion II; one with sub-monolayer dopant absorption but low mobility as I; and classes III–VI related to boundaries with increasing thickness, segregation and mobility.

In our study, WC–Al_2O_3 composites were codoped with MgO and CeO_2. As the ionic radii of Mg^{2+} (r_{Mg2+}= 0.072 nm) and Ce^{4+}/Ce^{3+} (r_{Ce4+}= 0.087 nm, r_{Ce3+}= 0.102 nm) were larger than that of W^{4+} and Al^{3+} (r_{W4+}= 0.066 nm, r_{Al3+}=0.053 nm), the solute misfit strain energy induced by large differences in ionic radii was the dominating driving force for the segregation of Mg and Ce ions to the grain boundaries. According to the theory of

Harmer [26], the oversized MgO and CeO_2 additives segregating to the grain boundaries effectively promoted the slow grain boundary transport; the MgO codoped with CeO_2 for size mixing to maximize the grain boundary complexion spacing filling could favor the formation of low mobility and stable boundary complexion types I or II, for which complexions, grain growth rate could be reduced due to the solute pinning effect.

When the MgO and CeO_2 additives were added, the complexions became defected and hence atomically roughened. This would result in normal grain growth (NGG). During the sintering process, grain boundary complexion transition may occur, in the faceted systems, there existed more than one type of growth behavior. According to the theoretical predictions and investigation of Kang et al. [28], the WC grain growth behavior and microstructural evolution during hot pressing could be investigated with respect to the variation of critical driving force (Δg_c) relative to the maximum driving force (Δg_{max}). The critical driving force is expressed as [29,30],

$$\Delta g_c = \frac{\pi\sigma^2}{kTh}(\ln K)^{-1} \quad (2)$$

Where σ is the free energy of the 2D nucleus, T is the sintering temperature, h is the height of the 2D nucleus, K is a constant that includes the diffusion coefficient and the number of nuclei per unit area. When $\Delta g_c = 0$, normal grain growth (NGG) occurs. For $0 < \Delta g_c \ll \Delta g_{max}$, Pseudo-NGG (PNGG) results. For $\Delta g_c \leq \Delta g_{max}$, conventional abnormal grain growth (AGG) occurs. For $\Delta g_c \gg \Delta g_{max}$, grain growth essentially does not occur (stagnant grain growth, SGG) [28].

In the undoped and doped WC–Al_2O_3 powder systems, the starting powder size and sintering conditions were the same, accordingly the change of Δg_{max} during the sintering was the same. The decrease of grain size in the MgO and CeO_2 doped WC–Al_2O_3 hot pressed samples were attributed to the effects of additives on the Δg_c.

As the particle size of as milled WC–Al_2O_3 powders were very small (47–573 nm), the average grain size at the initial stage of sintering was small and Δg_{max} may be much larger than Δg_c, the growth rate was governed by diffusion and the grain growth behavior was quite normal, in accordance with PNGG growth type.

With the sintering proceeded, for the undoped WC–Al_2O_3 composites, Δg_{max} decreased relative to Δg_c with grain growth, and Δg_{max} could then be close to Δg_c, some of the grains can grow appreciably, resulting in the formation of abnormal grains. However, for the WC–Al_2O_3 composites doped with MgO and CeO_2, ions segregated at grain boundaries, the interfaces were roughened and the step free energy was decreased, as a result, the Δg_c decreased, the relationship of Δg_c and Δg_{max} remained the state of $\Delta g_c \leq \Delta g_{max}$, PNGG occurred and no abnormal grain growth was observed. Dopant additions decreased the step free energy and inhibited the grain growth were also observed in the Al_2O_3 system with MgO addition [31], and VC and carbon doped WC–Co compound [32,33].

In addition, the movement of grain boundaries (WC–WC, Al_2O_3–Al_2O_3) were blocked by the CeO_2 additive segregating on the grain boundaries of WC–40 vol%Al_2O_3 composites, so that pores could not be trapped into the grains of WC–40 vol%Al_2O_3 composites. When the migration speed of grain boundaries (V_b) was equal to that of pores (V_p), pores would stay at grain boundaries all along and move altogether with them, and then get together rapidly and eliminate from grain and phase boundaries, which were the fast transfer channels of vacancy. As a result, grains of WC–40 vol%Al_2O_3 composites with almost no pores trapped in, become fine and compact. The increasing content of CeO_2 on the grain boundaries caused grain growth and resulted in the decrease of relative density. Accordingly, the mechanical properties decreased.

When the ions of the additives segregated in the WC–Al_2O_3 phase boundaries, due to the high surface activity, Ce ions could remove the gas absorbed on the surfaces of as-milled powders, reducing the residual pores in the phase boundaries, increasing the relative density of WC–Al_2O_3 composites. The activity of Ce could also result in the formation of some high melting point compounds with O and other impurity elements, purifying the phase boundaries. The composition of phase boundaries could be changed if Ce ions reacted with Al ions to form new compounds, the bonding strength of phase boundaries would be enhanced. When excess amount of additives were added, phase boundaries would be weakened, then the cracks may propagate along the phase boundaries, it would be harmful for the flexural strength; however, due to the increased crack propagation path, the fracture toughness may be increased slightly.

3.2. Summarize of mechanical properties of MgO and CeO_2 doped WC–40 vol%Al_2O_3 composites

To investigate the MgO and CeO_2 codoped effects on the properties of WC–40 vol%Al_2O_3 composites, the WC–40 vol%Al_2O_3 composites doped with MgO and CeO_2 together were hot pressed at 1540 °C for 90 min. Table 1 summaries the composition proportion and compares the mechanical properties of WC–40 vol%Al_2O_3 composites doped with MgO and CeO_2, both individually and together. The WC–40 vol%Al_2O_3, WC–40 vol%Al_2O_3–0.1 wt%MgO, WC–40 vol%Al_2O_3–0.1 wt%CeO_2, WC–40 vol%Al_2O_3–0.1 wt%MgO–0.1 wt%CeO_2 and WC–40 vol%Al_2O_3–0.05 wt%MgO–0.05 wt%CeO_2 composites would be referred to as WA, WA0.1M, WA0.1C, WA0.1M0.1C and WA0.05M0.05C, respectively, in Table 1 and the following text.

From Table 1, it could be seen that the decreased grain size of WC, and the increased Vickers hardness, fracture toughness and flexural strength could be achieved in the WA composites doped with 0.1 wt%MgO and 0.1 wt%CeO_2

Table 1
Composition proportion and mechanical properties of WC–40 vol%Al_2O_3 composites doped with MgO and CeO_2, both individually and together.

Powder system	Sintering process	Relative density (ρ%)	Grain size of WC (d_{WC})	Vickers hardness (HV_{30})	Fracture toughness (K_C)	Flexural strength (σ)
		%TD	μm	GPa	MPa $m^{1/2}$	MPa
WA		98.36 ± 0.08	3.92 ± 0.09	16.55 ± 0.25	8.52 ± 0.22	883.35 ± 23.41
WA0.1M	1540 °C	98.96 ± 0.15	2.30 ± 0.12	17.61 ± 0.17	9.59 ± 0.18	932.47 ± 18.96
WA0.1C	−90 min	98.82 ± 0.11	2.71 ± 0.14	16.89 ± 0.15	9.85 ± 0.14	1024.05 ± 24.39
WA0.1M0.1C	−39.6 MPa	98.10 ± 0.13	4.23 ± 0.26	16.54 ± 0.2	8.43 ± 0.16	872.49 ± 21.38
WA0.05M0.05C		99.04 ± 0.09	2.06 ± 0.12	18.18 ± 0.36	10.14 ± 0.25	1158.38 ± 23.05

separately, illustrating that proper amount of MgO and CeO_2 were beneficial to the properties of WA.

When adding 0.1 wt%MgO and 0.1 wt%CeO_2 together into the WA composites, the grain size of WC increased, the Vickers hardness, fracture toughness and flexural strength decreased compared with the undoped WA composites, indicating that when the WA composites codoped with 0.1 wt%MgO and 0.1 wt%CeO_2 together, the total amount of the additives exceeded the optimum amount, they would located at the grain boundaries as impurities, increasing the grain boundary width and leading to the coarsened grains and lowered density, resulting in the decreased mechanical properties.

The WA composites codoped with 0.05 wt%MgO and 0.05 wt%CeO_2 possessed a relative density of 99.04% and a smallest WC grain size of 1.86 μm, combining a highest Vickers hardness of 18.18 GPa with the excellent fracture toughness of 10.14 $MPa \cdot m^{1/2}$ and flexural strength of 1158.38 MPa. The MgO and CeO_2 additives occupying the intergranular positions exhibited a grain boundary pinning effect. The WC grain size of WA0.05M0.05C composites reduction was considered to be due to the formation of low mobility grain boundaries, which could result in the lowered porosity and high Vickers hardness. It was possible that the grain boundaries and microstructure of WA composites were changed in either chemistry or structure by the presence of the sintering aids of MgO and CeO_2, resulting in the decreased grain size of WC matrix and affecting the mechanical properties. The refined microstructure may change the crack extension mode, as analyzed in the following part of the paper, improving the fracture toughness of the WA composites. Generally, the strength of a polycrystalline ceramic material is determined by many factors that include chemical composition, microstructure and surface conditions [34]. The improvement of the flexure strength achieved in the WA0.05M0.05C composites as compared with that of undoped WA, MgO doped only and CeO_2 doped only WA composites, indicated that 0.05MgO and 0.05CeO_2 could increase the grain boundary fracture energy of the WA composites.

So it could be concluded that better doping effectiveness can be obtained for WA composites codoped with proper amount of MgO and CeO_2 compared with the WA composites doped with MgO and CeO_2 separately.

Besides the effects of additives, the residual thermal stress field could also result in variation of the mechanical properties of the sintered samples. As investigated in our previous work [9], for the MgO and CeO_2 doped WA composites, when the radius of the particulate (r) was small, both the radial tensile stress (σ_r) and tangential compressive stress (σ_t) were small [35], branches and deflection of cracks benefit to the increase of fracture toughness could be generated. With the increase of particle size, especially when the radius of a particulate was greater than the critical value, the particulate would be pulled off from the matrix by a large enough tensile stress (σ_r) [35], inducing microcracks at the interface. And the residual stress could reach a critical value as well, resulting in matrix microcracks that can be easily connected with each other upon external loading, reducing the fracture toughness of the material.

According to Taya et al. [36], the variation of fracture toughness caused by residual stress is

$$\Delta K_C = 2P_i\sqrt{\frac{2d(1.085\text{-}f_p^{1/2})}{f_p^{1/2}}} \quad (3)$$

Where d is the diameter of the particulates; f_p is the volume fraction of the particulates; From Eq. 5, it can be seen that, in the MgO and CeO_2 doped WA composites, with the decreasing particulates size, the variation of fracture toughness caused by residual stress would be reducing, the effect of residual stress on the fracture toughness become unconspicuous.

3.3. Analysis of the phases of MgO and CeO_2 doped WC–40 vol%Al_2O_3 composites

The effects of the addition of MgO and CeO_2 on the decarburization of WC and microstructure of WA, WA0.1M, WA0.1C and WA0.05M0.05C composites were compared and analyzed to reveal the reasons for improving mechanical properties and the toughening mechanism.

XRD patterns of the undoped WA, WA0.1M, WA0.1C and WA0.05M0.05C composites hot pressed at 1540 °C for 90 min were shown in Fig. 3. From Fig. 3a, it can be seen that, the phases of the undoped WA composites were WC, α-Al_2O_3, W_2C and C, indicating that WC was decarburized to C and W_2C due to the low degree of vacuum during the

sintering. The decarburization of WC to C and W_2C is thought to proceed in the following equation [37]:

$$2WC \rightarrow W_2C + C \quad (4)$$

The WC and Al_2O_3 powders were expected to contain air including oxygen during the stored process. When the powders were sintered under vacuum, the oxygen on the surface of the powders was reduced and carbon was consumed. Consequently, there was a lack of carbon to maintain the WC and WC was decarburized to W_2C. With the high hardness and low Young's modulus [38], W_2C was generally thought to be a brittle phase harmful to the properties of sintered composites. The suppression of decarburization of WC was essential to improve the mechanical properties of WA composites.

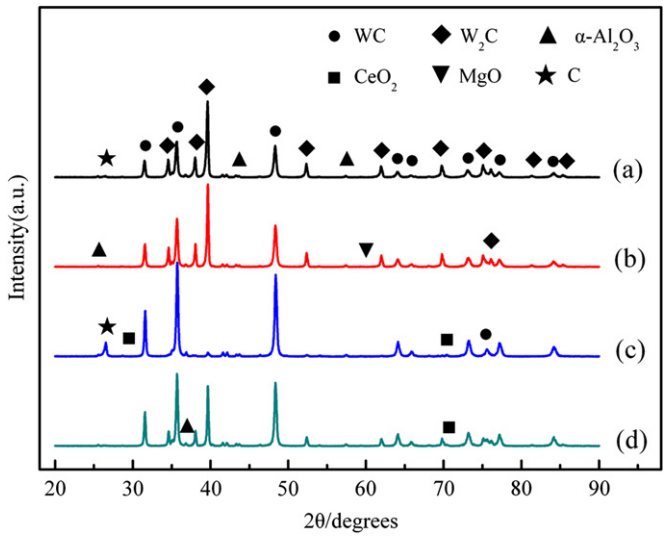

Fig. 3. XRD patterns of the (a) undoped WC–40 vol%Al_2O_3 composites and WC–40 vol%Al_2O_3 composites doped with (b) 0.1 wt% MgO, (c) 0.1 wt% CeO_2, (d) 0.05 wt% MgO and 0.05 wt% CeO_2 hot pressed at 1540 °C for 90 min.

When 0.1 wt%MgO were added to the WA composites, a similar XRD pattern was obtained, there was W_2C in the WA0.1M composites as well. A small peak of MgO and no other new phases were observed, as shown in Fig. 3b, indicating that MgO had no obvious effect on the suppression of decarburization of WC. According to the WC grain size and mechanical properties of WA0.1M shown in Table 1, it could be indicated that one of the obvious and important effects of MgO on the WA composites was inhibiting the grain growth of WC.

When 0.1 wt%CeO_2 were added to the WA composites, peaks of WC, α-Al_2O_3, CeO_2, W_2C and C were detected, according to its XRD pattern shown in Fig. 3c. The intensity of W_2C was very low compared with that of WA and WA0.1M composites, which could be observed in Fig. 3a and b, indicating that the decarburization suppression could be achieved with adding 0.1 wt%CeO_2 in the WC–40 vol%Al_2O_3 powders system. The suppression of decarburization no doubtfully could contribute to the

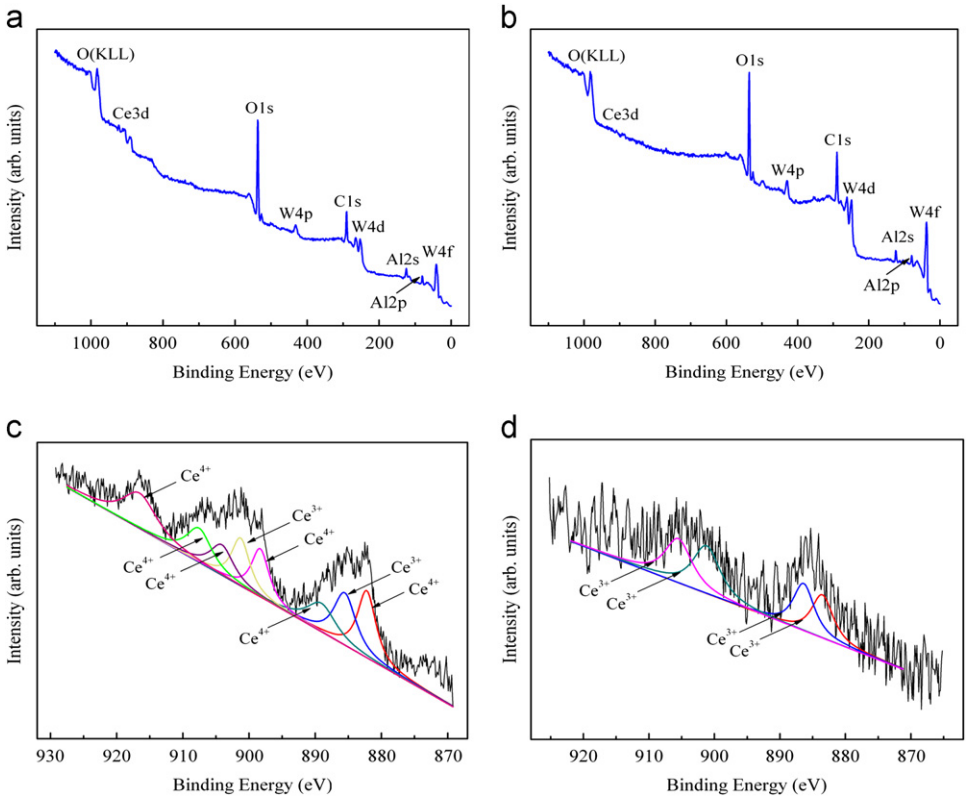

Fig. 4. XPS spectra of WC–40 vol%Al_2O_3–0.1 wt%CeO_2 (a) as milled powders and (b) hot pressed bulk composites, (c) high resolution spectra and peak fitting results of Ce element in (a), (d) high resolution spectra and peak fitting results of Ce element in (b).

improvement of mechanical properties. This was one of the reasons for the increase of Vickers hardness, fracture toughness and the flexural strength, as shown in Table 1. Peaks of the $CeAlO_3$ and $CeAl_{11}O_{18}$ were not observed in the XRD spectra. To investigate whether the CeO_2 was reduced to Ce_2O_3 to form some possible insoluble compounds, such as $CeAlO_3$ or $CeAl_{11}O_{18}$ phases [39,40], X-ray Photoelectron Spectroscopy (XPS) was carried out to confirm the presence of Ce^{3+}.

The XPS spectra of the WA0.1C as milled powders and hot pressed bulk composites were shown in Fig. 4a and b. The peaks of W, C, Al, O and Ce atoms were observed. The variations of Ce element were observed in the binding energy (BE) range of 865.20 eV to 929.20 eV. More detailed analysis of the Ce high resolution spectra of WA0.1C as milled powders and hot pressed bulk composites were presented in Fig. 4c and d.

In Fig. 4c, the peaks at 885.54 eV and 901.27 eV correspond to Ce^{3+} elements, while other peaks belonged to Ce^{4+} elements. It could be indicated that, besides the Ce^{4+}, there were a minor amount of Ce^{3+} in the WA0.1C as milled powders. The Ce^{3+} may come from the original CeO_2 powders. However, none peaks of Ce^{4+} were observed and all the peaks were assigned to Ce^{3+} in the XPS spectra of the hot pressed bulk composites, as shown in Fig.4d, indicating that all the Ce^{4+} elements were reduced to Ce^{3+}. The transformation of Ce^{4+} to Ce^{3+} verified that some compounds actually formed in the WC–Al_2O_3 phase boundaries and Al_2O_3-Al_2O_3 grain boundaries, greatly improving the bonding strength of the composites.

From Fig.3d, it can be indicated that, the WA0.05M0.05C composites were mainly composed of the WC, α-Al_2O_3 and W_2C phases. The intensities of MgO and CeO_2 were very low due to the small amount of them. Although the W_2C peaks still were detected, the intensities of them were lower than that of WA and WA0.1 M composites, indicating that the decreased amount of W_2C was due to the suppression effect of CeO_2 contained in the WA0.05M0.05C composites and the mechanical properties of WA0.05M0.05C composites were the result of the comprehensive effect of MgO and CeO_2.

3.4. Analysis of the microstructure of MgO and CeO_2 doped WC–40 vol% Al_2O_3 composites

Representative microstructure of the polished WA, WA0.1M, WA0.1C and WA0.05M0.05C composites were shown in Fig. 5. According to the EDS analysis, the grey region contrasts Al_2O_3 and the bright region contrasts matrix WC. Comparing Fig. 5b–d with Fig. 5a, it can be seen that the dispersion morphologies and the particle size of the Al_2O_3 toughening particulates were significantly influenced by the MgO and CeO_2 additions. Without the additives, the Al_2O_3 particulates showed an irregular polygonal shape and a particle size of 1.94 μm, measured using five images similar with Fig. 5a. However, the Al_2O_3 toughening particulates in the hot pressed WA composites with additions of MgO and CeO_2 both individually and together were presented in refined and dispersed morphology (as shown in Fig. 5b–d). The Al_2O_3 particle size of the WA0.1M, WA0.1C and WA0.05M0.05C composites were 1.42 μm, 1.63 μm and 1.09 μm, respectively, which were much smaller than that of the undoped WA composites, indicating that both MgO and CeO_2 could affect the dispersion states and the size of

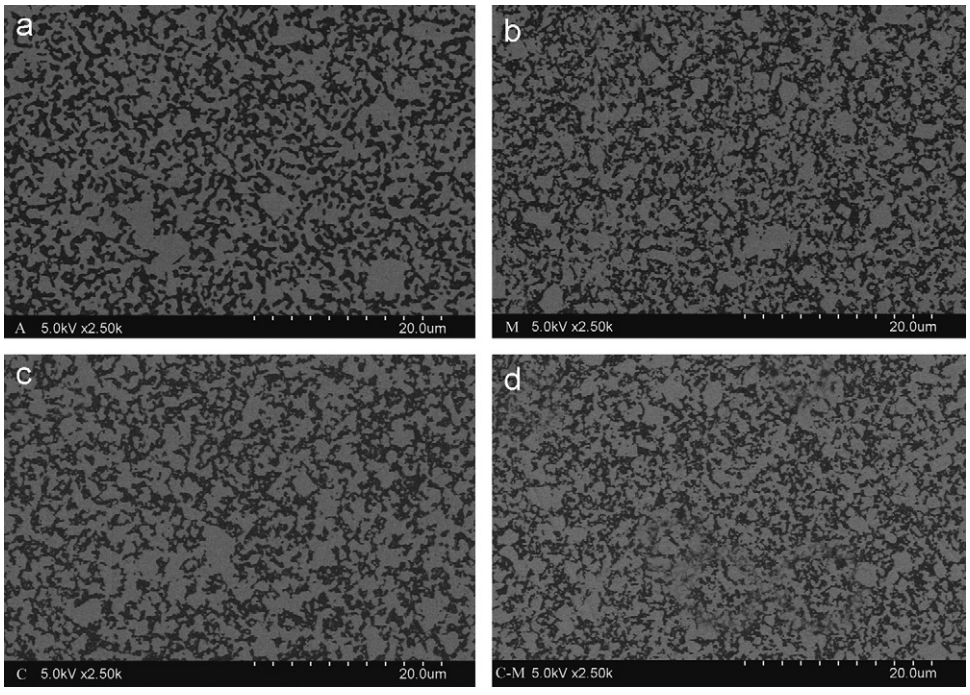

Fig. 5. FE-SEM images of the polished (a) undoped WC–40 vol%Al_2O_3 composites and WC–40 vol%Al_2O_3 composites doped with (b) 0.1 wt% MgO, (c) 0.1 wt% CeO_2, (d) 0.05 wt% MgO and 0.05 wt% CeO_2 hot pressed at 1540 °C for 90 min.

Al_2O_3 toughening particulates; the inhibiting effect to the Al_2O_3 particle size of MgO was much better than that of CeO_2, and the optimum microstructure and the inhibiting effect were achieved in the WA composite doped with MgO and CeO_2 together. This could be used to explain the best mechanical properties determined by the microstructure of the WA0.05M0.05C composites.

The characteristic microstructures of the polished and etched samples are shown in Fig. 6. A number of SEM photos similar to that of Fig. 6 were used to evaluate the grain size of WC matrix. With no additions, the WC grains of WA composites were significantly coarsened, which were 3.92 μm in size, as shown in Fig. 6a. However, the refined WC matrix grains were visibly observed with a corresponding addition of MgO and CeO_2, separately or together, as shown in Fig. 6b–d. The WC matrix grain size of the WA0.05M0.05C composites was 1.86 μm smaller than that of the WA0.1M and WA0.1C composites (2.3 μm and 2.71 μm). It could be revealed that both the type and amount of the additives were important factors of the hot pressing of WA composites.

Fig. 7 shows the FE-SEM images of the Vickers indentation crack extension paths of WA, WA0.1M, WA0.1C and WA0.05M0.05C composites. The fracture toughness was a property that materials resisted to the propagating of cracks, so the toughening mechanism could be analyzed on the basis of the crack paths microstructure. From Fig. 7a, it can be seen that, although there were some small crack deflections, the crack of WA composites was relatively straight with a larger width, indicating that the undoped microstructure cannot absorb the energy of cracks and prevent crack propagation effectively. So the fracture toughness was low. From Fig. 7b–d, it can be observed that the width of cracks decreased and the amount of crack deflections increased. As a result, the fracture toughness increased compared with that of the undoped WA compoaites. From Fig. 7b-A and b-B, it could be seen that the crack extended along the interfaces of WC and Al_2O_3 in the WA0.1M composites, that is, the fracture of WA0.1M composites would be intergranular mode. It could be indicated that those boundaries may be relatively weak compared with the grains, however, crack extending along the particle interfaces could increase the length of crack propagation path, as a result, the fracture toughness was improved. Cracks propagation breaking the WC matrix were observed in the WA0.1C composites, as shown in Fig. 7c-A, B and C, absorbing much more energy than that of crack deflections along the interfaces, resulting in the higher fracture toughness and flexural strength than that of the WA0.1 M composites. Fig. 7d shows a secondary crack pattern in the WA0.05M0.05C composites. A secondary crack is a crack branching pattern of a main crack, generating during the indentation crack extension due to the equivalent tensile stress value in different directions. The generation and existence of the secondary crack could consume the energy of the main crack. In addition, crack deflections and crack propagation breaking the WC matrix were observed as well. It could be indicated that addition of 0.05MgO and 0.05CeO_2 had greatly improved the bonding conditions of the grain boundaries and the interfaces around WC grains were

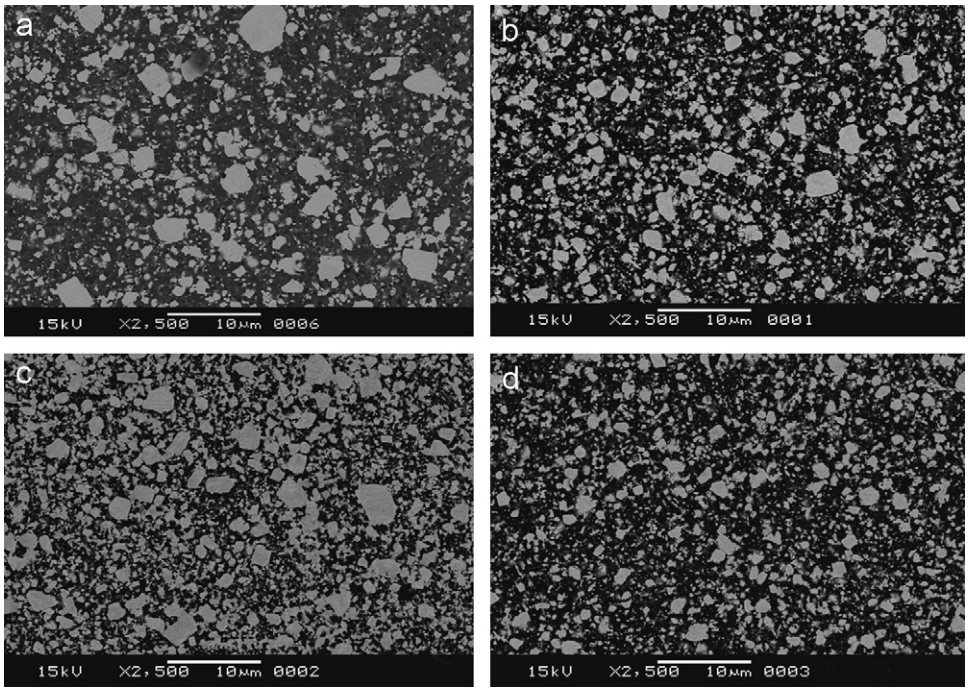

Fig. 6. SEM images of the polished and etched (a) undoped WC–40 vol%Al_2O_3 composites and WC–40 vol%Al_2O_3 composites doped with (b) 0.1 wt% MgO, (c) 0.1 wt% CeO_2, (d) 0.05 wt% MgO and 0.05 wt% CeO_2 hot pressed at 1540 °C for 90 min.

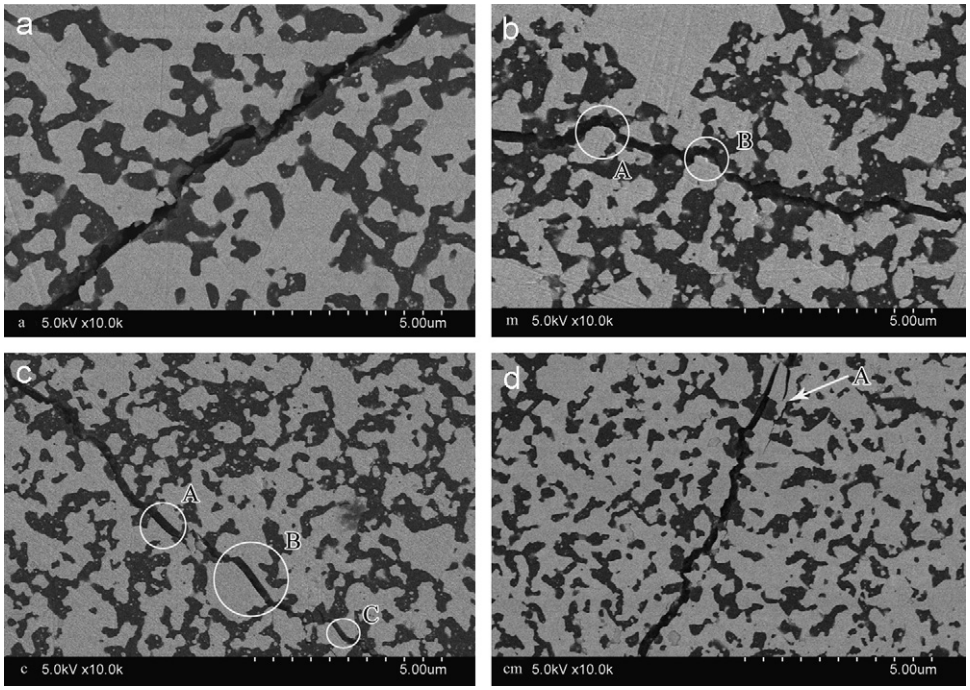

Fig. 7. FE-SEM images of Vickers indentation crack extension path of (a) undoped WC–40 vol%Al_2O_3 composites and WC–40 vol%Al_2O_3 composites doped with (b) 0.1 wt% MgO, (c) 0.1 wt% CeO_2, (d) 0.05 wt% MgO and 0.05 wt% CeO_2 hot pressed at 1540 °C for 90 min.

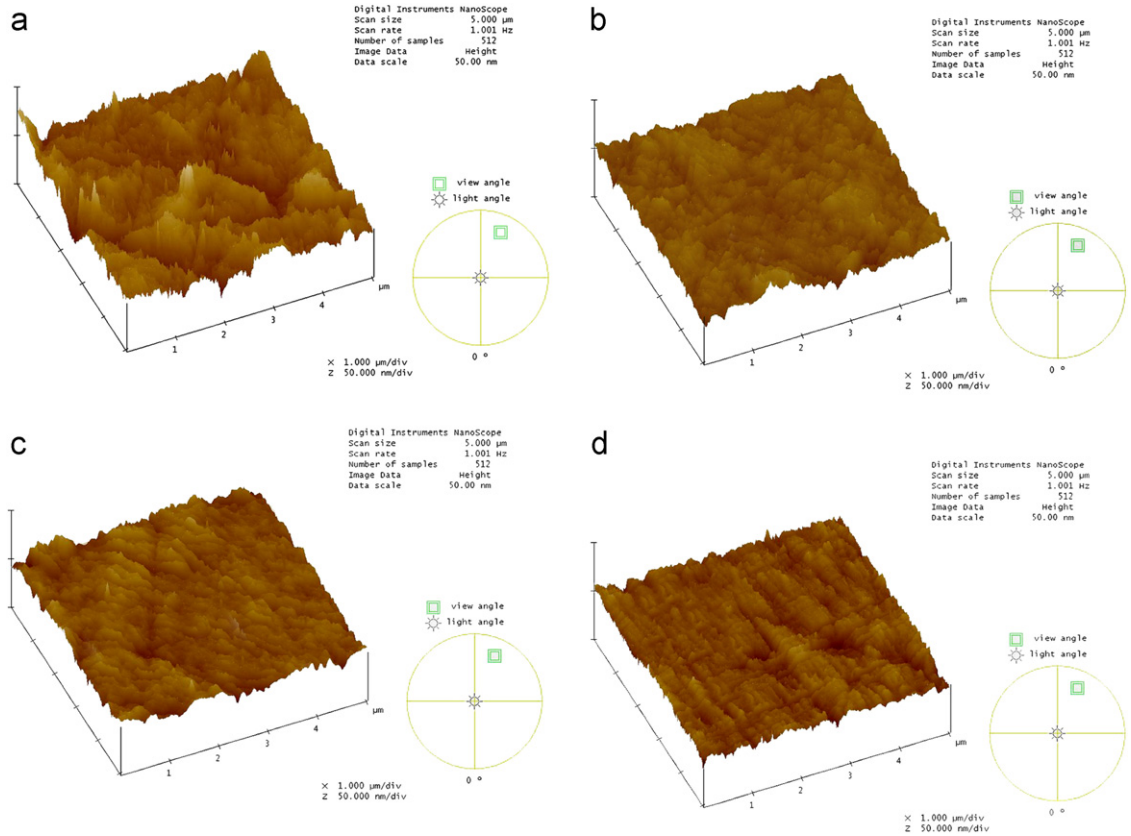

Fig. 8. 3D SPM images showing the particulate/matrix interfacial microstructures of (a) undoped WC–40 vol%Al_2O_3 composites and WC–40 vol%Al_2O_3 composites doped with (b) 0.1 wt% MgO, (c) 0.1 wt% CeO_2, (d) 0.05 wt% MgO and 0.05 wt% CeO_2 hot pressed at 1540 °C for 90 min.

sufficiently strong that the crack avoided those diversions. Crack growth was prevented and the fracture toughness and flexural strength would be significantly improved.

When MgO and CeO_2 were added in the WA composites, they would accumulate along the grain boundaries, refining the microstructure and resulting in more crack deflections

and bridges. The crack bridge link behavior and the crack interacting effect between the matrix and toughening particulates might lead to the formation of coexisting field of crack deflection, crack branch and crack bridge, interlacing with each other during extension of cracks to form a kind of complex pattern of crack extension, absorbing much of the energy of crack expansion, leading to the enormously improvement of fracture toughness and flexural strength.

Fig. 8 shows the particulate/matrix interfacial microstructures in the hot pressed samples of WA composites without and with MgO and CeO_2 added. The test samples were ground and polished with diamond paste to 0.05 μm surface finish, the polished surface was also cleaned with acetone for the characterization. It could be seen that the morphology of undoped WA composites was rough and fluctuated, as shown in Fig. 8a, which may due to the large and incompletely separated Al_2O_3 toughening particulates. From Fig. 8b–d, it could be seen that the particulate/matrix interfacial combining morphologies of WA doped with 0.1M, 0.1C and 0.05M 0.05C, respectively, were much more smooth, indicating that the Al_2O_3 toughening particulates in these composites had the continuous and compatible interfaces with the matrix, predicting that the synergistic effect of MgO and CeO_2 could increase the fracture toughness and the flexural strength.

4. Conclusions

(1) WC–40 vol%Al_2O_3 composite powders doped with MgO and CeO_2, both separately and together, could be consolidated by hot pressing at 1540 °C for 90 min under a pressure of 39.6 MPa.
(2) The additions of 0.1 wt%MgO, 0.1 wt%CeO_2 and 0.05 wt%MgO0.05 wt%CeO_2 in the WC–Al_2O_3 composites could promote the microstructural refinement and improve the interface coherence of the WC matrix and Al_2O_3 leading to the enhancement of the mechanical properties.
(3) Trace MgO mainly acted as an effective grain growth inhibitor for the WC–Al_2O_3 composites and trace CeO_2 could suppress the decarburization of WC as well due to the unique properties of rare earth elements such as high surface activity and large ionic radius.
(4) The synergistic effect of 0.05 wt%MgO and 0.05 wt%CeO_2 added in WC–Al_2O_3 composites resulted in the achievement of a relative density of 99.04% with an excellent Vickers hardness of 18.18 GPa, combining a fracture toughness of 10.14 MPa $m^{1/2}$ with an acceptable flexural strength of 1158.38 MPa. Excessive addition of MgO and CeO_2 (0.1 wt%MgO and 0.1 wt%CeO_2) could deteriorate the mechanical properties of the WC–Al_2O_3 composites.

Acknowledgments

The authors would like to acknowledge the financial support provided by Shanghai Leading Academic Discipline Project under Project no: B602, and the support by the Nanomaterials Research Special Foundation of Shanghai Science and Technology Committee under Grant no: 05nm05031.

References

[1] F.A. Deorsola, D. Vallauri, G.A. Ortigoza Villalba, B.D. Benedetti, Densification of ultrafine WC–12Co cermets by pressure assisted fast electric sintering, International Journal of Refractory Metals and Hard Materials 28 (2010) 254–259.
[2] H.C. Kim, I.J. Shon, J.E. Garay, Z.A. Munir, Consolidation and properties of binderless sub-micron tungsten carbide by field-activated sintering, International Journal of Refractory Metals and Hard Materials 22 (2004) 257–264.
[3] H.C. Kim, I.J. Shon, J.K. Yoon, J.M. Doh, Consolidation of ultra fine WC and WC–Co hard materials by pulsed current activated sintering and its mechanical properties, International Journal of Refractory Metals and Hard Materials 25 (2007) 46–52.
[4] H.C. Kim, D.K. Kim, K.D. Woo, I.Y. Ko, I.J. Shon, Consolidation of binderless WC–TiC by high frequency induction heating sintering, International Journal of Refractory Metals and Hard Materials 26 (2008) 48–54.
[5] O. Malek, B. Lauwers, Y. Perez, P.D. Baets, J. Vleugels, Processing of ultrafine ZrO_2 toughened WC composites, Journal of The European Ceramic Society 29 (2009) 3371–3378.
[6] S.G. Huang, O. Van der Biest, J. Vleugels, Pulsed electric current sintered Fe_3Al bonded WC composites, International Journal of Refractory Metals and Hard Materials 27 (2009) 1019–1023.
[7] M.L. Zhang, S.G. Zhu, J. Ma, C.X. Wu, Preparation of WC/MgO composite nanopowders by high energy reactive ball milling and their plasma activated sintering, Powder Metallurgy and Metallic Ceramics 47 (2008) 525–530.
[8] C.X. Wu, S.G. Zhu, J. Ma, M.L. Zhang, Synthesis and formation mechanisms of nanocomposite WC–MgO powders by high-energy reactive milling, Journal of Alloys and Compounds 478 (2009) 615–619.
[9] H.X. Qu, S.G. Zhu, Q. Li, C.X. Ouyang, Influence of sintering temperature and holding time on the densification, phase transformation, microstructure and properties of hot pressing WC–40 vol%Al_2O_3 composites, Ceramics International 38 (2012) 1371–1380.
[10] R.L. Coble, Sintering crystalline solids II. Experimental test of diffusion models in porous compacts, Journal of applied physics 32 (5) (1961) 793–799.
[11] S.J. Bennison., M.P. Harmer, A history of the role of MgO in the sintering of α alumina, in: C.A. Handwerker, J.E. Blendell, W.A. Kaysser (Eds.), Sintering of Advanced Ceramics, OH, Westerville, 1990, pp. 13–49.
[12] K.A. Berry, M.P. Harmer, Effect of MgO solute on microstructure development in Al_2O_3, Journal of the American Ceramic Society 69 (2) (1985) 143–149.
[13] K. Yan, T. Meng, T. Yu, The effect on mechanical properties and cutting performances of cemented carbide inserted with rare earth metal elements, Journal of Southwest Jiaotong University 30 (1995) 46–51.
[14] Q.F. Pan, Effects of rare earth oxides on the properties of WC–Co cemented carbide, Rare Metal Materials and Engineering 22 (1993) 35–41.
[15] D.H. Xiao, Y.H. He, M. Song, N. Lin, R.F. Zhang, Y_2O_3- and NbC-doped ultrafine WC–10Co alloys by low pressure sintering, International Journal of Refractory Metals and Hard Materials 28 (2010) 407–411.
[16] J. Ma, S.G. Zhu, P. Di, Y. Zhang, Influence of La_2O_3 addition on hardness, flexural strength and microstructure of hot-pressing sintered WC–MgO bulk composites, Materials and design 32 (2011) 2125–2129.

[17] Y. Takigawa, Y. Ikuhara, T. Sakuma, Grain boundary bonding state and fracture energy in small amount of oxide doped fine grained Al2O3, Journal of Materials Science 34 (1999) 1991–1997.
[18] H. Endo, M. Ueki, Hot-pressing and Pressureless Sintering of WC–Al_2O_3 Ceramic Composites, Transactions of the Materials Research Society of Japan 16B (1994) 819–822.
[19] D.K. Shetty, I.G. Wright, P.N. Mincer, A.H. Clauer, Indentation fracture of WC–Co cermets, Journal of Materials Science 20 (1985) 1873–1882.
[20] Z.Y. Deng, Y. Zhou, M.E. Brito, Y. Tanaka, T. Ohji, Effects of rare earth dopants on grain boundary bonding in alumina–silicon carbide composites, Journal of the European Ceramic Society 24 (2004) 511–516.
[21] I.P. Shapiro, R.I. Todd, J.M. Titchmsrsh, S.G. Roberts, Effects of Y_2O_3 additives and powder purity on the densification and grain boundary composition of Al_2O_3/SiC nanocomposites, Journal of the European Ceramic Society 29 (2009) 1613–1624.
[22] W.D. Kingery, Plausible concepts necessary and sufficient for interpretation of ceramic grain boundary phenomena:I. grain boundary characteristics, structure, and electrostatic potential, Journal of the American Ceramic Society 57 (1974) 1–8.
[23] H.K. Schmid, R. Pennefather, Redistribution of Ce and La during processing of Ce(La)–TZP/Al_2O_3 composites, Journal of the European Ceramic Society 10 (1992) 381–392.
[24] C.W. Li, W.D. Kingery, Solute segregation at grain boundaries in polycrystalline Al_2O_3, Advances in Ceramics 10 (1984) 368–378.
[25] C.H. Su, Q.D. Duanmu, Y. Wang, Nbn-equilibrium thermodynamic analysis of the concentration distribution of rare earth oxide at alumina transparent ceramic crystal boundary, Journal of the Chinese Ceramic Society 26 (6) (1998) 802–807.
[26] M.P. Harmer, Interfacial kinetic engineering: how far have we come since Kingery's inauhural sosman address?, Journal of the American Ceramic Society 93 (2) (2010) 301–317
[27] S.J. Dillon, M.P. Harmer, Demystifying the role of sintering additives with complexion, Journal of the European Ceramic Society 28 (2008) 1458–1493.
[28] S.J.L. Kang, M.G. Lee, S.M. An, Microstructural evolution during sintering with control of the interface structure, Journal of the American Ceramic Society 92 (7) (2009) 1464–1471.
[29] W.K. Burton, N. Carbrera, F.C. Frank, The growth of crystals and the equilibrium structure of their surface, Philosophical Transactions of the Royal Society of London A243 (1951) 299–358.
[30] D.Y. Yoon, C.W. Park, J.B. Koo, in: H. Yoo, S.J.L. Kang (Eds.), The Step Growth Hypothesis for Abnormal Grain Growth, Vol. 2, Institute of Materials, London, 2001, pp. 3–21.
[31] C.W. Park, D.Y. Yoon, Abnormal grain growth in alumina with anorthite liquid and the effect of MgO addition, Journal of the American Ceramic Society 85 (6) (2002) 1585–1593.
[32] T. Yamamoto, Y. Ikuhara, T. Sakuma, High resolution transmission electron microscopy study in VC-doped WC–Co compound, Science and Technology of Advanced Materials 1 (2000) 97–104.
[33] I. Sugiyama, M. Goto, T. Taniuchi, F. Shirase, T. Tanase, K. Okada, Y. Ikuhara, T. Yamamoto, Blunt corners of WC grains induced by lowering carbon content in WC–12mass%Co cemented carbides, Journal of Materials Science 46 (2011) 4413–4419.
[34] W.F. Smith, in: Foundations of Materials Science and Engineering, 4th ed., China Machine Press, Beijing, 2005.
[35] T. Mari, K. Tanaka, Average stress in matrix and average elastic energy of materials with misfitting inclusions, Acta Metallurgica 21 (1973) 571–574.
[36] M. Taya, S. Hayashi, A.S. Kobayashi, Toughening of a particulate reinforced ceramic matrix composite by thermal residual stress, Journal of the American Ceramics Society 73(5): 1382–1391.
[37] M.E. Vinayo, F. Kassabji, J. Guyonnet, P. Fauchais, Plasma sprayed WC–Co coatings: Influence of spray conditions (atmospheric and low pressure plasma spraying) on the crystal structure, porosity, and hardness, Journal of Vacuum Science and Technology A, 3 (6) (1985) 2483–2489.
[38] H. Taimatsu, S. Sugiyama, Y. Kodaira, Synthesis of W_2C by reactive hot pressing and its mechanical properties, Materials Transactions 49 (2008) 1256–1261.
[39] J.Z. Shyu, W.H. Weber, H.S. Gandhi, Surface characterization of alumina supported ceria, Journal of Physical Chemistry 92 (1988) 4964–4970.
[40] S. Damyanova, C.A. Perez, M. Schmal, J.M.C. Bueno, Characterization of eria-coated alumina carrier, Applied Catalysis A-General 234 (2002) 271–282.